




## Exploring the Impact of Digital Reform on Music Education in Colleges and Universities

Huihui Ji<sup>1\*</sup> 

<sup>1</sup>Xinyang Vocational and Technical College, Xinyang, 464000, China

Corresponding author: Huihui Ji, [huihuiji45@yahoo.com](mailto:huihuiji45@yahoo.com)

**Abstract.** In order to improve the effect of music education in colleges and universities, this paper conducts digital processing of college music education resources through digital technology, and analyzes the resonance characteristics and working mechanism of half-wavelength SIR. Furthermore, this paper explains the principle of the transmission zero point generated by the feeding structure from the field and microwave theory point of view, and proposes a band-pass filter with transmission zero point. In addition, this paper embeds a band-pass filter with transmission zero into the microstrip feeder of DRA to improve the effect of digital music processing, and design experiments to verify the effect of the system proposed in this paper. Through the experimental research results, it can be seen that the digital system of music education resources in colleges and universities proposed in this paper has a good effect.

**Keywords:** data governance; college music; educational resources; digitization.

**DOI:** <https://doi.org/10.14733/cadaps.2023.S9.114-130>

### 1 INTRODUCTION

Music digitization technology is a real-time information interaction technology based on computer technology and Internet technology, covering the processing and dissemination of music digitized information such as sound, picture, text, and data. First of all, in the classroom application of music digital technology, a multi-audio-visual interactive teaching method can be realized, which greatly enriches the teaching content of the classroom. In the music teaching classroom, the teaching content not only includes the sound display of music, but also the teaching display of text and images such as music scores and music performances. The application of digital music digital technology in music classroom can greatly expand the teaching content of music classroom. In addition, music digital technology also includes the penetration of Internet technology. The application of music digitalization in music classrooms also connects the space of music classrooms with the Internet space. In the vast space of the Internet, there are not only a large number of music resources, but also a public discussion space for various music exchanges, which provides a large number of teaching resources and teaching content for music classrooms.

The teaching of music digital technology is a teaching method based on computer technology. Teachers only need to introduce computers, audio and screen projection equipment in the classroom to carry out teaching activities [1]. Moreover, in the teaching process of music digital technology, thanks to the help of computer screen projection, teachers only need to prepare in advance the text, audio, pictures, etc. required for teaching, and make PPT and other display courseware for teaching. In addition, the teaching of music digital technology is different from the traditional teaching method. It does not require teachers to spend time writing on the blackboard in the classroom, which greatly saves the teaching and writing time and greatly improves the efficiency of the classroom [2]. In the music teaching classroom, teachers can organize music scores and other text teaching content into electronic documents and present them in PPT and other forms in advance, without the need to display them on the blackboard. At the same time, when showing music cases in the classroom, teachers can also obtain case resources through online search to explain, without leaving the supplementary content for the next class. Therefore, with the help of music digital technology, the efficiency of music classroom can be significantly improved [3].

The teaching content of music digital technology connects massive Internet resources with the classroom, providing teachers with a large number of dynamic resources. In the process of rapid development of computer information technology, the Internet has undergone iterations of Web1.0, Web2.0, and Web3.0, and various online music resources are constantly being updated and developed. A large number of text, audio, and image resources such as music scores, music audio, and live music performances have been stored in the Internet [4]. In the music teaching classroom, teachers can arbitrarily mobilize the teaching resources of the digital music end at any time. At the same time, music production software was also developed on the computer side. A large number of modern and digital music production software resources have emerged in the Internet. In the teaching of music classroom, teachers can even use the music production software provided by Internet resources through the music digital terminal to realize the on-site music production teaching in the classroom only by the computer system [5]. Through the music resources of music digital computer technology, teachers can greatly improve the classroom atmosphere and stimulate students' interest in learning [6].

In the teaching process of music classroom, digital music information technology is only a teaching tool for teachers. How to play the value of music digital technology in music classroom requires teachers to fully study and practice. Music digitization technology covers a variety of media technologies such as text, sound, image, animation, etc., and these technologies can be matched in different ways according to needs to achieve the best communication effect [7]. However, this is also the difficulty of using music digitization technology in teaching. How to teach with different media technologies also needs to follow the principles of music digitization. The principle of music digitalization does not mean that all media interaction methods are carried out in the classroom, but it needs to be matched with the teaching content and the best music digitalization method should be used. For example, when a teacher explains a certain classical score, he can make a text courseware of the score to show it, and at the same time enjoy the audio or video of the performance of the score. In addition, teachers can also use the music production software on the computer side to perform live music scores, and give full play to the advantages of music digital technology [8].

In the application of music digitalization in classroom teaching, music teachers need to follow the principle of moderation on the basis of the principle of music digitalization. The application of digital music technology in music teaching does not force teachers to use digital music tools for classroom explanations. Traditional music teaching methods cannot be completely replaced by music digital technology [9]. For example, although the process of writing music scores on the blackboard will take more time than the music digitization technology, in fact, as teachers write music symbols on the blackboard, stroke by stroke, it is also an effective way for the students to gain memory time, students can more easily remember the content of the class in the blackboard. In addition, although the audio-visual technology of music digitization can show students a more realistic music scene, it is not advisable to simply play music videos in the classroom. This can easily make students feel burnout, lose their attention, and reduce the quality of classroom teaching [10].

With the advancement of digital technology, the digital transformation of teaching resources has both economic and social benefits. Dynamic teaching resources are a new type of teaching resources generated in the digital learning environment. Schools with conditions should encourage teachers and technicians Use information tools to meet the learning needs of learners. The following principles should be followed in the design of digital resources: starting from the learning needs of students, taking learning as the leading role, and building a space that can be continuously enriched and updated, building digital teaching resources with "flow generation", and allowing students to actively participate in the resources. Come. Constructing an information-based interactive learning environment is more attractive and effective for teaching [11]. To overcome the defects of technology and teaching gap in the previous digital teaching resource design process, teachers and students can dynamically add new content at any time, so that technology can be harmoniously integrated into teaching [12]. The specific design of digital teaching resources. Doing a good job in the teaching design of online courses is the key to the development of online courses. It is expected that students will further deepen their learning. The teaching content refers to the integration of learners' systematic learning knowledge, skills and behavioral experience in order to achieve teaching goals. According to the requirements of teaching objectives, the teaching content of this course is established, and the teaching content is decomposed into relatively independent knowledge structures [13]. All activities of instructional design are to promote the learning of learners, and all activities of instructional design are to promote the learning of learners. They are experience-based, problem-solving as the center, and have a high psychological self-awareness and Self-motivation and self-evaluation ability. Use visual teaching to adapt to students' intuitive thinking mode [14]. For specific teaching content, in a specific teaching situation, the comprehensive emphasis of special students is creative ability, which involves the conceptualization of value and the organization of value systems, and perceptual skills, which refer to the observation of stimuli in the environment. And understanding, determine the video courseware mainly explained by teachers, so that learners do not feel lonely in the learning process, so that learners can master various learning management software through learning. Media refers to the vivid, intuitive and image of information in the process of transmission, which can better help learners understand the teaching content and combine abstract problems with practice. Evaluation and revision are important contents in the teaching design process. It is usually carried out after the teaching activities, and the purpose is to investigate the teaching objectives [15].

In order to improve the effect of music education in colleges and universities, this paper uses digital technology to carry out digital processing of music education resources in colleges and universities, and improve the quality of intelligent processing of music education resources in colleges and universities.

## 2 MUSIC WAVEFORM ALGORITHM ANALYSIS

### 2.1 Theoretical Analysis of Rectangular Dielectric Resonator Antenna

Due to the edge boundary problem of dielectric resonators, the dielectric waveguide model is generally used for the analysis of rectangular dielectric resonators. As shown in Figure 1, the guided wavelength in a rectangular cross-section dielectric waveguide is calculated by using the dielectric waveguide model. As shown in Fig. 1(a), we assume that the rectangular cross-section of the model has length  $a$  in the  $x$ -axis direction and  $b$  in the  $y$ -axis direction. Electromagnetic waves propagate in the  $z$ -axis direction and the  $z$ -axis direction is infinitely long. The field inside the dielectric waveguide can be divided into  $TE'_{mn}$  and  $TM_m$  modes. Among them,  $m$  and  $n$  respectively represent the number of wavelengths of the electromagnetic wave in the  $x$ -axis and  $y$ -axis directions in the dielectric waveguide, and  $y$  represents the electromagnetic wave propagates along the  $y$ -axis direction. As shown in Figure 1(b), the inner field of the rectangular dielectric waveguide varies sinusoidally, while the outer field varies exponentially with decay. Meanwhile, for the convenience of analysis, the electric field of the shaded part in Fig. 1(b) is assumed to be 0.

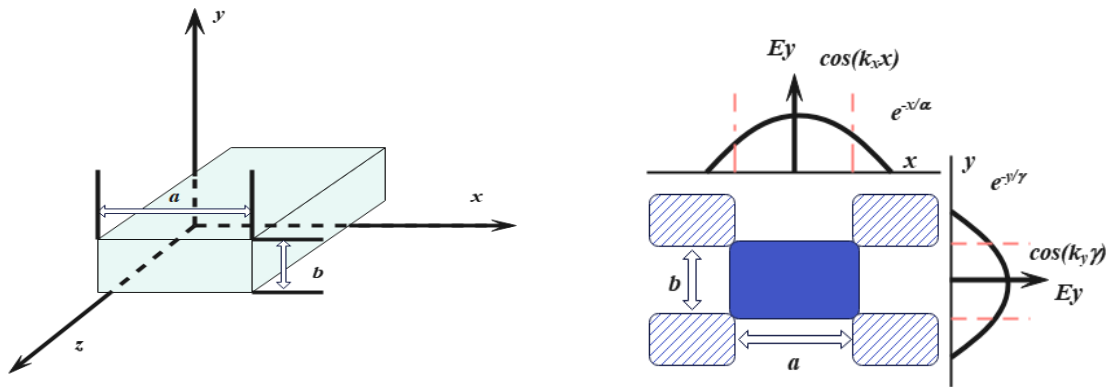


**Figure 1:** Rectangular dielectric waveguide model (a)Medium wave-guide model diagram, (b)Cross-sectional field distribution diagram.

In the range of  $|x| \leq a/2$  and  $|y| \leq a/2$ , the propagation of electromagnetic waves in the x-axis, y-axis and z-axis directions are represented by  $k_x$ ,  $k_y$  and  $k_z$ , respectively. In the range of  $|x| \geq a/2$  and  $|y| \geq b/2$ , the attenuation coefficients of electromagnetic waves in the x-axis and z-axis directions are represented by  $\alpha$  and  $\gamma$ , respectively. According to the field of boundary conditions, they are:

$$\begin{aligned}
 k_z &= \sqrt{\epsilon_r k_0^2 - k_x^2 - k_y^2} \\
 k_x &= \frac{m\pi}{a} \left( 1 + \frac{2}{ak_0\sqrt{\epsilon_r - 1}} \right)^{-1} \\
 k_y &= \frac{n\pi}{b} \left( 1 + \frac{2}{bk_0\sqrt{\epsilon_r - 1}} \right)^{-1} \\
 \alpha &= \frac{1}{\sqrt{(\epsilon_r - 1)k_0^2 - k_x^2}} \\
 \gamma &= \frac{1}{\sqrt{(\epsilon_r - 1)k_0^2 - k_y^2}}
 \end{aligned} \tag{1}$$

Among them,  $k_0$  is the wave number in free space, and its size is:

$$k_0 = \frac{2\pi}{\lambda_0} = \frac{2\pi f}{c} \tag{2}$$

Among them,  $\lambda_0$  is the wavelength corresponding to the working frequency in free space,  $f_0$  is the working frequency, and  $c$  is the speed of light in vacuum. If we assume ideal magnetic walls at  $x = \pm a/2$ ,  $y = \pm b/2$ ,  $k_x$  and  $k_y$  can be approximated as:

$$k_x = \frac{m\pi}{a}$$

$$k_y = \frac{n\pi}{b}$$
(3)

The infinitely long dielectric waveguide in Figure 1 is truncated in the  $z$ -axis direction, and it is assumed that the truncated surface is an ideal magnetic wall, so an isolated DRA model suitable for free space is obtained, as shown in Figure 2(a). If the rectangular DRA is placed on the metal ground, due to the mirror image principle, the height of the dielectric resonator is 1/2 of that in isolation, as shown in Figure 2(b).

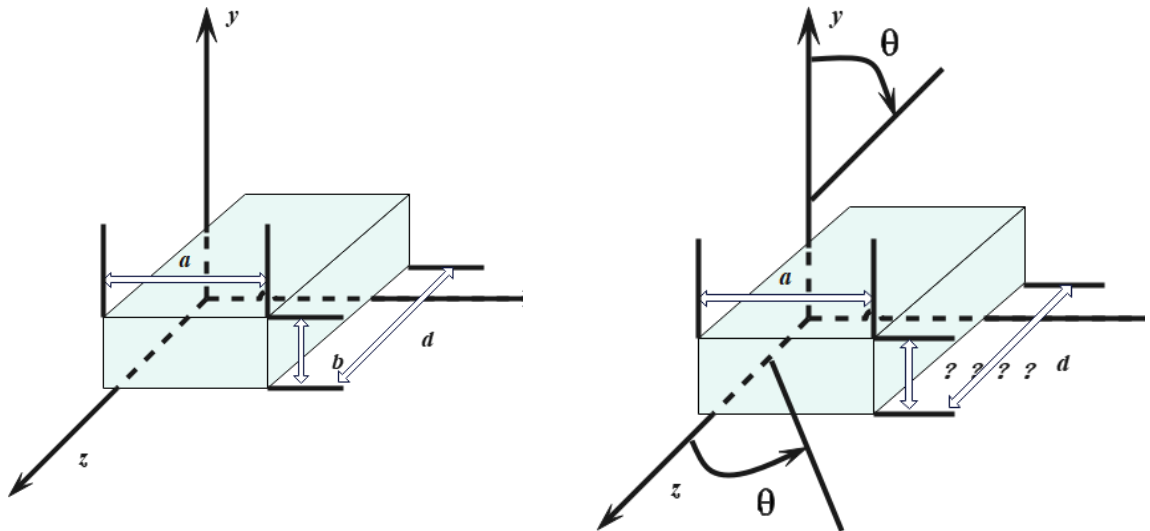


**Figure 2:** Rectangular dielectric waveguide and rectangular DRA model (a) The truncated dielectric waveguide (b) Rectangular DRA placed on the metal ground.

When there is  $a, b > d$ , the fundamental mode of the rectangular DRA is  $TE_{n15}$ , the dielectric waveguide model is utilized, and the field in this mode can be expressed as:

$$H_x = \frac{(k_x k_z)}{j\omega\mu_0} \sin(k_x x) \cos(k_y y) \sin(k_z z)$$
(4)

$$H_y = \frac{(k_y k_z)}{j\omega\mu_0} \cos(k_x x) \cos(k_y y) \sin(k_z z)$$
(5)

$$H_z = \frac{(k_x^2 k_z^2)}{j\omega\mu_0} \cos(k_x x) \cos(k_y y) \cos(k_z z) \quad (6)$$

$$E_x = k_y \cos(k_x x) \sin(k_y y) \cos(k_z z) \quad (7)$$

$$E_y = -k_x \sin(k_x x) \cos(k_y y) \cos(k_z z) \quad (8)$$

$$E_z = 0 \quad (9)$$

Among them, there is

$$k_x^2 + k_y^2 + k_z^2 = \varepsilon_r k_0^2 \quad (10)$$

$$k_z \tan(k_z d / 2) = \sqrt{(\varepsilon_r - 1)k_0^2 - k_z^2} \quad (11)$$

Through the above analysis, the rectangular dielectric waveguide model is utilized, and the resonant frequency of the rectangular DRA placed on the ground can be calculated by the following formula:

$$f_0 = \frac{c}{2\pi\sqrt{\varepsilon_r}} \sqrt{k_x^2 + k_y^2 + k_z^2} \quad (12)$$

$$k_x = \frac{m\pi}{a} \quad (13)$$

$$k_z = \frac{n\pi}{2b} \quad (14)$$

$$d = \frac{2}{k_y} \tanh\left(\frac{k_{y0}}{k_y}\right), k_{y0} = \sqrt{k_x^2 + k_y^2} \quad (15)$$

Meanwhile, the relative bandwidth of DRA can be calculated by the following formula:

$$BW = \frac{S-1}{\sqrt{SQ}} \quad (16)$$

Among them, S is the maximum incident voltage standing wave ratio (VSWR), and Q is the quality factor of the antenna.

## 2.2 Mode Field Distribution and Radiation Characteristics of Rectangular Dielectric Resonator Antennas

In order to better describe the variation of the field along the x-axis, y-axis and z-axis in a rectangular DRA, TE<sub>mp</sub> is usually used to represent the mode of the field. Among them, the superscript y represents the rectangular waveguide assumed to propagate along the y-axis direction, the subscript m represents the wave number of the field along the x-axis direction, the subscript n represents the wave number of the field along the y-axis direction, and the subscript p represents the field along the z-axis direction wave number in the axial direction. As shown in Figure 3, it is the

electric and magnetic field distributions of the fundamental mode TE<sup>y</sup><sub>11</sub> and higher-order modes TE<sup>y</sup><sub>2</sub> and TE<sup>y</sup><sub>13</sub> of an isolated rectangular DRA. The electromagnetic simulation software HFSS16.0 is used to simulate the electric field distribution of the rectangular DRA, as shown in Figure 4.

When the rectangular DRA is placed on a metal ground, the height of the rectangular dielectric resonator is reduced by half due to the mirror effect of the ground. At the same time, the higher-order mode TE<sup>y</sup><sub>2</sub> cannot be excited. Figure 5 shows the electric and magnetic field distributions for a rectangular DRA placed on a metal ground. Figure 6 shows the simulated electric field distribution of the fundamental mode TE<sup>y</sup><sub>11</sub> and the higher-order mode TE<sup>y</sup><sub>13</sub> of the rectangular DRA.

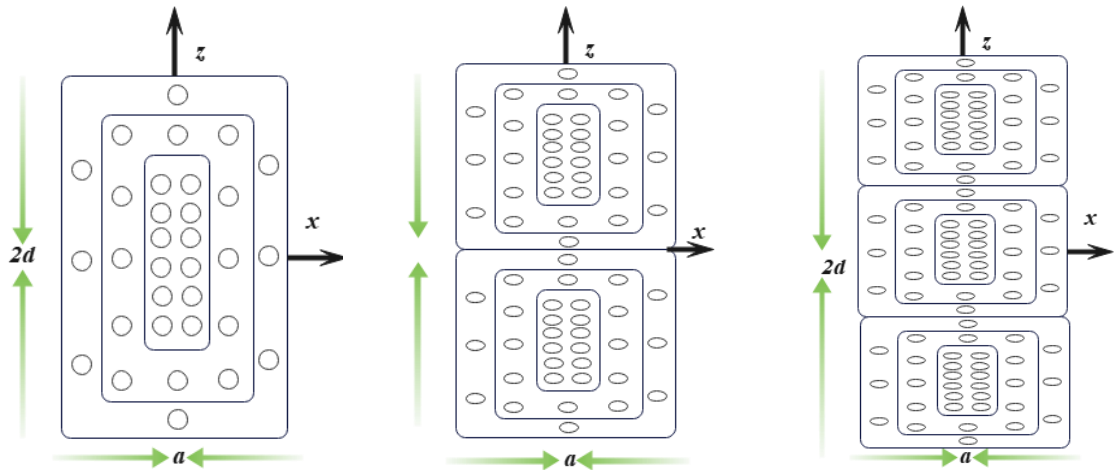


**Figure 3:** Field distribution of an isolated rectangular DRA (electric field is solid line; magnetic field is dots and  $\times$ ) (a)TE<sup>y</sup><sub>11</sub> model, (b)TE<sup>y</sup><sub>12</sub> model, (c)TE<sup>y</sup><sub>13</sub> model.

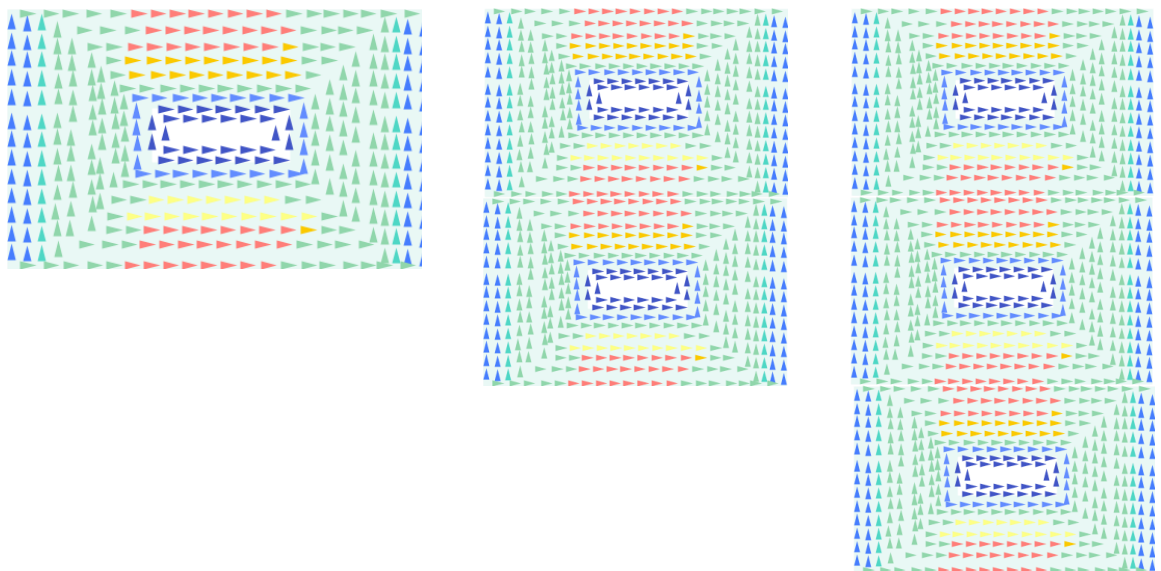


**Figure 4:** Isolated DRA simulated electric field distribution (a)TE<sup>y</sup><sub>11</sub> model, (b)TE<sup>y</sup><sub>12</sub> model, (c) TE<sup>y</sup><sub>13</sub> model.

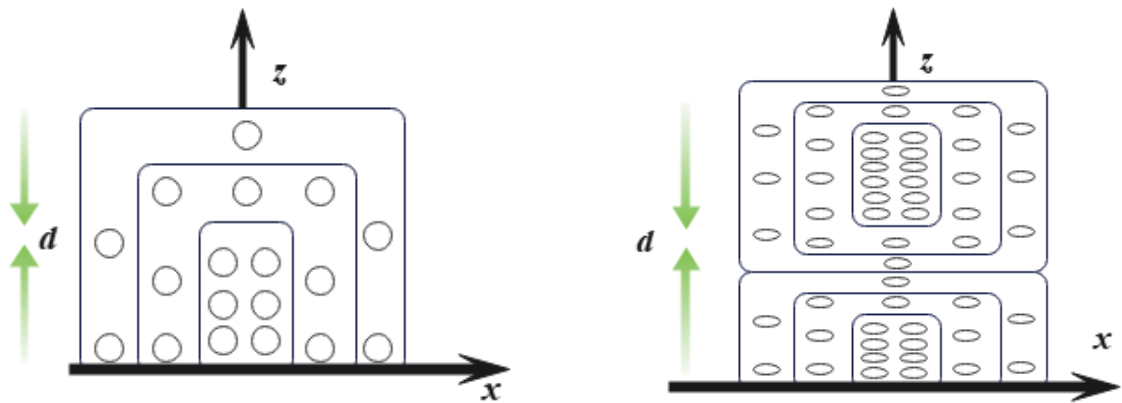


**Figure 5:** Field distribution of a DRA placed on the ground (electric field is solid line; magnetic field is dots and  $\times$ ) (a) $TE^y_{111}$  model, (b) $TE^y_{113}$  model.

The field distribution of the lowest-order mode of a rectangular DRA is similar to that of a magnetic dipole, which can be calculated by the dielectric waveguide model formulation. Therefore, the radiation pattern of the DRA can be equivalent using a magnetic dipole. As shown in Figure 7, the equivalent model of the  $TE^y_{111}$  and  $TE^y_{113}$  modes of a rectangular DRA placed on the ground is equivalent to the horizontal magnetic dipoles aligned along the y-axis direction. It is worth mentioning that due to the superposition of the original magnetic dipole and the imaged magnetic dipole, the size of the resultant magnetic dipole at  $Z=0$  is twice that of the original dipole. In order to reduce the beamwidth with side lobes, the separation of the two magnetic dipoles is about  $s = 0.4\lambda_0$  ( $\lambda_0$  is the guided wavelength of free space). As a result, the DRA heights of the  $TE^y_{111}$ -mode and  $TE^y_{113}$ -mode are approximately  $\lambda_0/3$  and  $\lambda_0/2$ , respectively. Moreover, it has been found that the gain of the higher order mode is higher than that of the fundamental mode. Therefore, the use of higher-order modes to design high-gain DRAs has attracted more and more attention. In addition, compared with other gain enhancement methods, this method has the advantages of simple structure and small volume, which meets the development requirements of modern wireless communication systems.

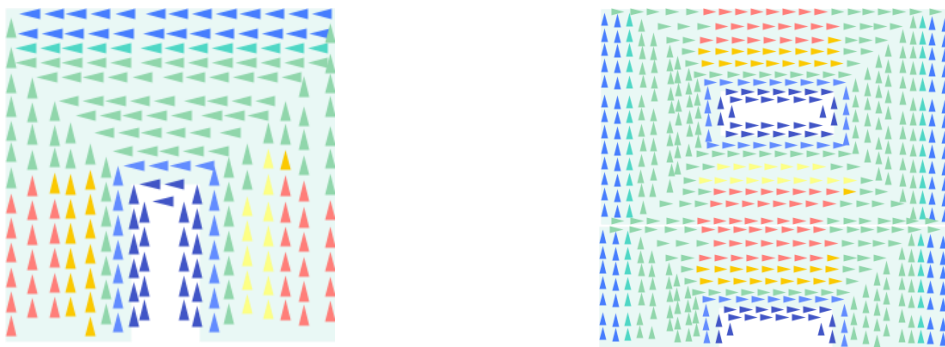


**Figure 6:** Simulated electric field distribution of a DRA placed on the ground (a) $TE^y_{111}$  model, (b) $TE^y_{113}$  model.



### 2.3 Filtered Dielectric Resonator Antenna based on Stepped Impedance Resonator

A design scheme of filtering DRA based on Stepped Impedance Resonator (SIR) operating at 3.5GHz is proposed. A band-pass filter with transmission zero is designed by analyzing the resonance characteristics of the SIR structure and the zero-degree feeding mode. Then, according to the filter synthesis design method, the filter with transmission zero is embedded in the 50Ω microstrip feeder of the rectangular DRA, as the feed network of the DRA, to realize the filtering function. At the same time, due to the generation of two radiation nulls on both sides of the passband, high out-of-band selectivity is provided for the antenna. In this design, the rectangular DR not only acts as a radiator to radiate energy, but also acts as the last-order resonator of the bandpass filter, thereby greatly reducing the overall size of the antenna.

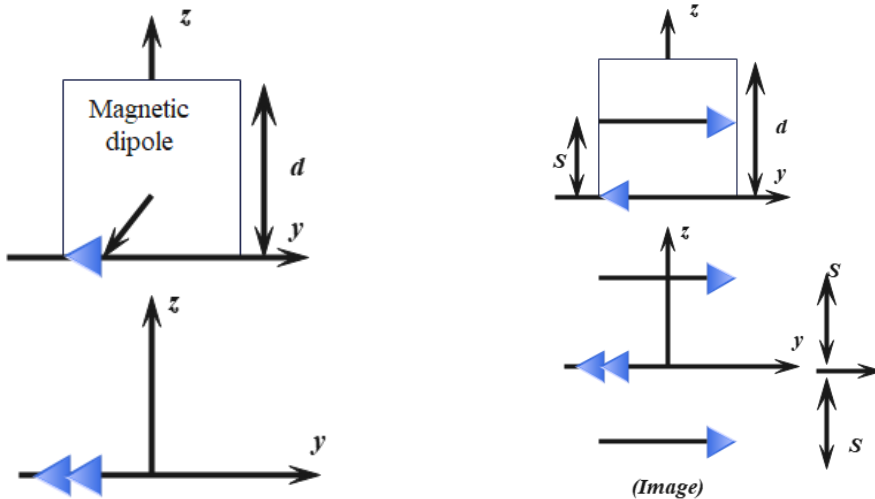


**Figure 7:** Equivalent magnetic dipole of DRA (a)TE<sub>111</sub> model, (b)TE<sub>1113</sub> model.

The SIR consists of two or more transmission lines with different characteristic impedances. It can reduce the size without changing the unloaded quality factor, which is beneficial to the design of the filter miniaturization. Moreover, its stray resonance frequency is controllable by adjusting its impedance ratio and electrical length ratio, which solves the problem of harmonic suppression of the filter very well. According to different electrical length, SIR can be divided into full-wavelength type, half-wavelength type, quarter-wavelength type.

The half-wavelength type SIR is utilized to design a bandpass filter, as shown in Figure 8. Half-wavelength SIR consists of uniform microstrip transmission lines with impedances  $Z_1$  and  $Z_2$  (corresponding electrical lengths  $\theta_1$  and  $\theta_2$ , respectively). Among them, the total electrical length of SIR is  $\theta_1 + \theta_2 = \pi$ . Impedance ratio and electrical length ratio are important characteristic parameters of SIR, which can be expressed by the following formula:

$$R_z = \frac{Z_2}{Z_1} \quad (17)$$

$$\alpha = \frac{\theta_2}{\theta_1 + \theta_2} \quad (18)$$

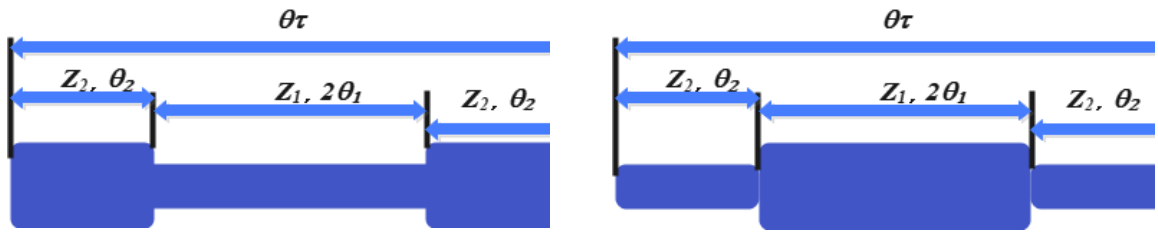


**Figure 8:** Schematic diagram of two structures of one-half wavelength SIR: (a)  $R_z < 1$ , (b)  $R_z > 1$ .

As shown in Figure 8, the input admittance seen from the open end of the SIR can be expressed as:

$$Y_i = jY_2 \frac{2(R_z \tan \theta_1 + \tan \theta_2)(R_z - \tan \theta_1 \tan \theta_2)}{R_z(1 - \tan^2 \theta_1)(1 - \tan^2 \theta_2) - 2(1 + R_z^2) \tan \theta_1 \tan \theta_2} \quad (19)$$

According to the resonance condition of the resonator  $Y_i = 0$ , the resonance condition of the SIR can be expressed as:

$$K = \tan \theta_1 \tan \theta_2 \text{ or } K \tan \theta_1 = -\tan \theta_2 \quad (20)$$

As can be seen from the formula, the resonance characteristics of the half-wavelength type SIR are determined by the impedance ratio  $R_z$  and the electrical lengths  $\theta_1$  and  $\theta_2$ . For the convenience of analysis and calculation, we assume  $\theta_1 = \theta_2 = \theta$ , and then formula (19) can be simplified as:

$$Y_i = jY_2 \frac{2(1 + R_z)(R_z - \tan^2 \theta) \tan \theta}{R_z - 2(1 + R_z + R_z^2) \tan \theta} \quad (21)$$

The resonance conditions are:

$$\theta = \arctan(\sqrt{R_z}) \quad (22)$$

We assume that the basic resonant frequency of the half-wavelength SIR is  $f_0$ , and the stray resonant frequency of each order is  $f_{SB1}$ ,  $f_{SB2}$ ,  $f_{SB3}$ , then the corresponding  $\theta$  is  $\theta_{S1}$ ,  $\theta_{S2}$ ,  $\theta_{S3}$ , which can be obtained from formula (21):

$$\begin{aligned} \theta_{S1} &= \pi/2 \\ \theta_{S2} &= \arctan(-\sqrt{R_z}) = \pi - \theta \\ \theta_{S3} &= \pi \end{aligned} \quad (23)$$

Therefore, the spurious resonant frequencies of the half-wavelength SIRs can be expressed as:

$$\frac{f_{SB1}}{f_0} = \frac{\theta_{S1}}{\theta} = \frac{\pi}{2 \arctan \sqrt{R_z}}$$

$$\frac{f_{SB2}}{f_0} = \frac{\theta_{S2}}{\theta} = 2 \left( \frac{f_{SB1}}{f_0} \right) - 1 \quad (24)$$

$$\frac{f_{SB3}}{f_0} = \frac{\theta_{S3}}{\theta} = 2 \left( \frac{f_{SB1}}{f_0} \right)$$

To sum up, when the SIR design bandpass filter is adopted, its stray resonance frequency can be adjusted according to the design performance index of the filter to achieve a good passband or improve the out-of-band characteristics. After each resonance frequency is determined, the corresponding impedance ratio and electrical length are obtained according to formula (3-8), and then the appropriate impedance value is selected according to the system requirements. Finally, the overall size of the half-wavelength SIR is determined from the corresponding wavelength and impedance calculations.

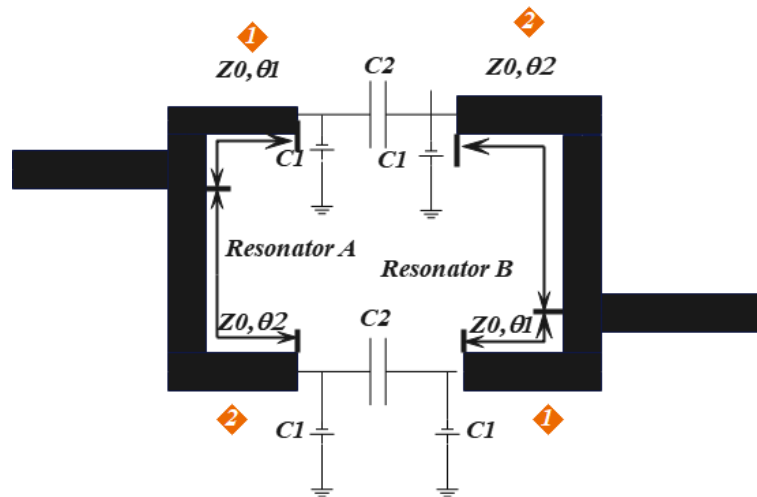


**Figure 9:** Zero-degree feed structure.

In order to explain the working mechanism of the zero-degree feeding structure to generate the transmission zero, the field analysis and theoretical derivation are explained respectively. As shown in Figure 9, in terms of field analysis, since there is no direct coupling between the transmission lines (1) with the same electrical parameters in resonator A and resonator B. When the signal is transmitted from resonator A to resonator B, the field strengths of the two cancel each other out, thus A transmission zero is generated.

From the theoretical derivation, the gap coupling between resonator A and resonator B is equivalently analyzed by an n-type capacitive network. Due to the lower frequency range of operation, the effect of  $\text{oC}_i$  is negligible.

Through the method of solving the transmission matrix analysis, the transmission matrices of the upper and lower channels (1) and (2) of the feed point are respectively:

$$\begin{pmatrix} A_u & B_u \\ C_u & D_u \end{pmatrix} = \begin{pmatrix} \cos(\theta_1 + \theta_2) + \frac{Y_0}{\omega C_2} \cos \theta_1 + \cos \theta_2 & jZ_0 \sin(\theta_1 + \theta_2) - i \frac{\cos \theta_1 \cos \theta_2}{\omega C_2} \\ jY_0 \sin(\theta_1 + \theta_2) - j \frac{Y_0^2}{\omega C_2} \sin \theta_1 \sin \theta_2 & \cos(\theta_1 + \theta_2) + \frac{Y_0}{\omega C_2} \sin \theta_1 \cos \theta_2 \end{pmatrix} \quad (25)$$

$$\begin{pmatrix} A_i & B_i \\ C_i & D_i \end{pmatrix} = \begin{pmatrix} \cos(\theta_1 + \theta_2) + \frac{Y_0}{\omega C_2} \sin \theta_1 \cos \theta_2 & jZ_0 \sin(\theta_1 + \theta_2) - j \frac{\cos \theta_1 \cos \theta_2}{\omega C_2} \\ jY_0 \sin(\theta_1 + \theta_2) - j \frac{Y_0^2}{\omega C_2} \sin \theta_1 \sin \theta_2 & \cos(\theta_1 + \theta_2) + \frac{Y_0}{\omega C_2} \cos \theta_1 \sin \theta_2 \end{pmatrix} \quad (26)$$

From the above transmission matrix,  $A_u + A_i = D_u + D_i$ ,  $B_u = B_i$  and  $C_u = C_i$  can be derived, so the transmission matrix can be simplified as:

$$\begin{pmatrix} A & B \\ C & D \end{pmatrix} = \begin{pmatrix} \frac{A_u + A_i}{2} & \frac{B_u}{2} \\ \frac{(A_u + A_i)^2 - 4}{2B_u} & \frac{A_u + A_i}{2} \end{pmatrix} \quad (27)$$

According to microwave theory, the network parameters are converted into S-parameter matrix, and  $S_{21}$  can be expressed as:

$$S_{21} = \frac{2}{A + B/Z_L + CZ_L + D} = \frac{4B_u Z_L}{B_u^2 + [2(A_u + A_i)^2 - 4]Z_L^2} \quad (28)$$

The condition for transmitting zero is  $B_u=0$ . Therefore, the production condition can also be expressed as:

$$\tan \theta_1 + \tan \theta_2 = 1/Z_0 \omega C_2 \quad (29)$$

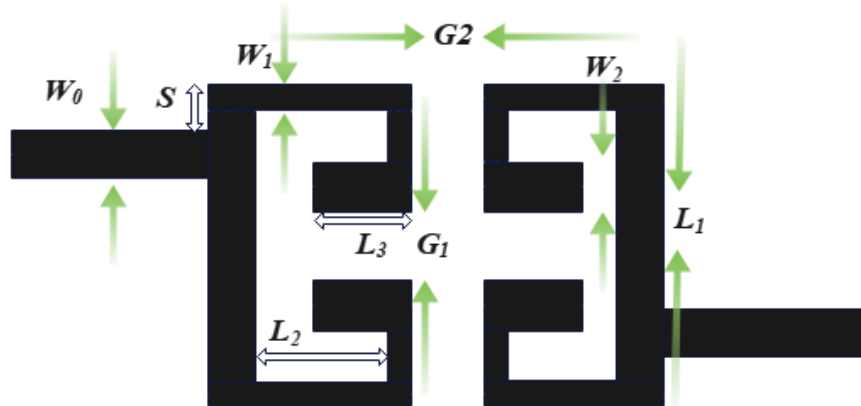
When the operating frequency is low, the value of  $C_3$  is usually 0.1pF or less, resulting in a large value of  $1/Z_0 \omega C_2$ . The relative bandwidth of bandpass filter design is usually in the range of 2%-12%. In order to obtain the required on-load quality factor, the electrical length in the resonator is generally designed in the  $1.2\theta_1 - 1.8\theta_2$  range. Formula (29) can be simplified as:

$$\tan \theta_1 \approx 1/Z_0 \omega C_2 \text{ or } \tan \theta_2 \approx 1/Z_0 \omega C_2 \quad (30)$$

Because the value of  $C_2$  is very small, the generation condition of the transmission zero is:

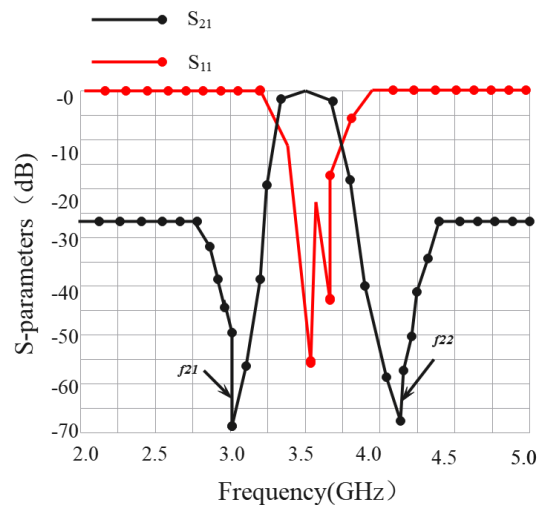
$$\theta_1 \approx \pi/2 \text{ or } \tan \theta_2 \approx \pi/2 \quad (31)$$

To sum up, the resonant frequency of the transmission zero point generated by the zero-degree feeding method is the corresponding frequency point when  $\theta_1$  and  $\theta_2$  outside the passband are close to  $\pi/2$ .



**Figure 10:** Schematic diagram of the proposed filter structure.

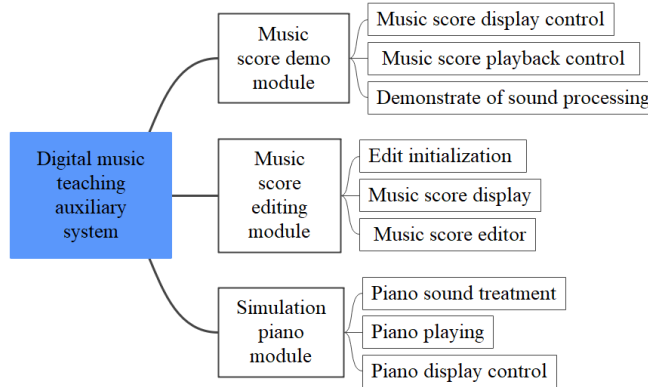
Based on the above analysis of half-wavelength SIR and zero-point feeding, a band-pass filter with transmission zero is proposed. Figure 10 is a structural diagram of the proposed band-pass filter, which adopts the coupling mode of zero-degree feeding. The microstrip SIR was printed on a dielectric substrate with a relative permittivity of 4.4 and a thickness of 0.762 mm. A 50 $\Omega$  microstrip feeder with a width of  $W_0$  is located at the input and output ends, and the input and output ends are center-symmetrical. The impedances of the different microstrip lines of the bent SIR are  $Z_1 = 56.03\Omega(W_1)$  and  $Z_2 = 69.4\Omega(W_2)$ , respectively, and the impedance ratio is  $R=0.807$ . S-parameters of the simulation is shown in Figure 11.



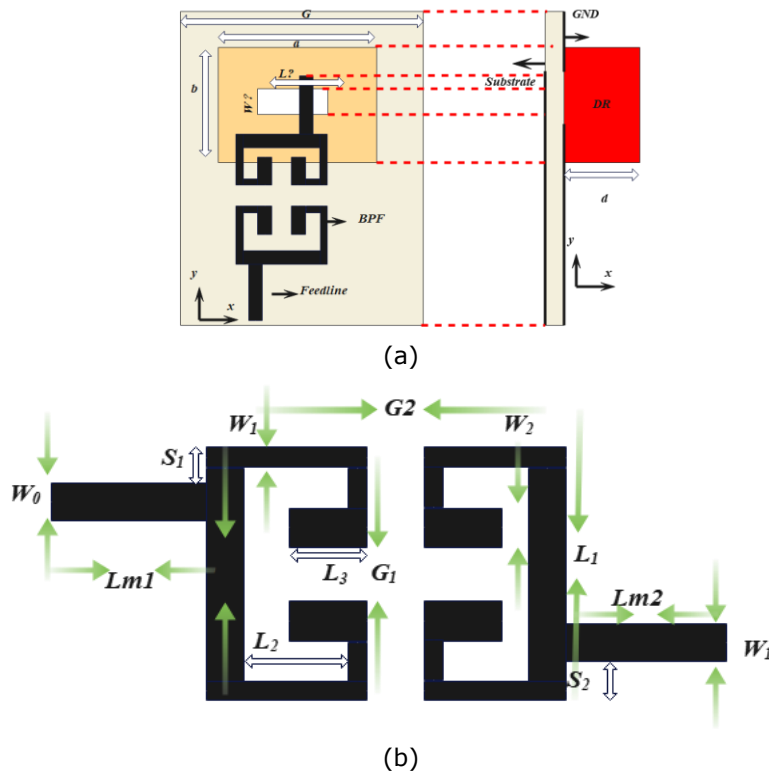
**Figure 11:** S-parameters of the simulation.

### 3 DIGITAL PROCESSING OF MUSIC EDUCATIONAL RESOURCES IN COLLEGE AND UNIVERSITIES

Since the system involves multiple modules, and each module contains multiple functions, in order to smoothly realize the coordinated operation among the modules in the system and the overall function, while ensuring the stability of the system and the expansion of later functions, the overall design of the system is specially designed. The overall module of the system is shown in Figure 12.



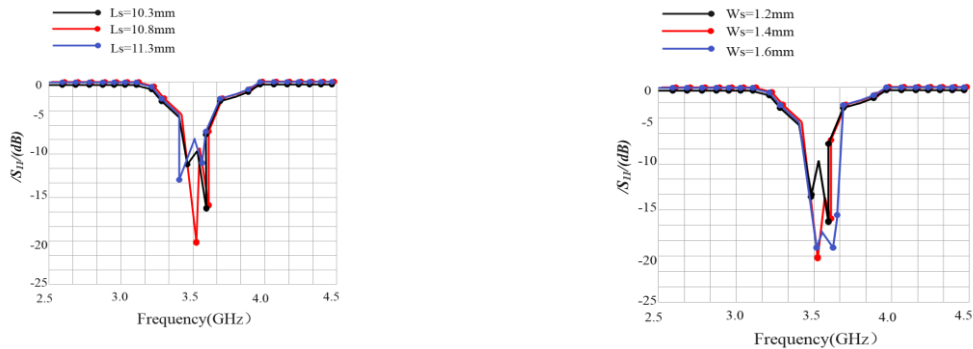
**Figure 12:** Overall system module.



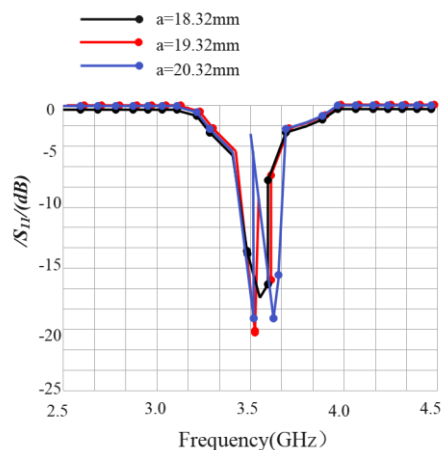
**Figure 13:** SIR-based filtering DRA structure diagram: (a) top (b) side views.

Figure 13 is a structural topology diagram of the proposed filter antenna. As shown in Fig. 13(a), the proposed antenna consists of a rectangular DR and a feeding circuit on a dielectric substrate. The rectangular DR with a relative permittivity of 10 is fed through a microstrip feed line through a coupling slot line. The length and width of the dielectric substrate are  $G$ , the thickness is 0.762 mm, and the relative permittivity is 4.4. At the same time, a filter with transmission null is embedded in the 50 microstrip feeder, providing high out-of-band frequency selectivity to the antenna.

In order to achieve a good impedance matching effect, the working frequency band of the DRA is consistent with the working frequency band of the filter. The SIR filter is embedded in the 50 $\Omega$  microstrip feeder as a part of the feed network of the DRA to excite the TEM mode of the DRA. The length and width of the coupling slot line are important parameters for adjusting the coupling coefficient between the bandpass filter and the DR. Therefore, in order to analyze the influence of the length and width of the coupling slot line on the coupling coefficient, the parameters of  $L$  and  $W$  were respectively swept. As shown in Figure 14(a), it can be seen that by changing the size of the coupling slot line, the impedance bandwidth of the antenna can be adjusted, and at the same time, the anti-matching effect of the antenna impedance can be affected. The proposed antenna has two resonance modes, among which the second resonance mode is due to the TE mode of the DRA. As shown in Figure 14(b), as the length  $a$  of the DR increases, the resonant frequency of the DRA gradually decreases. Variation curve of  $S$  parameter with  $a$  is shown in Figure 15.



**Figure 14:** S parameter change curve. (a)Ls (b)Ws.



**Figure 15:** Variation curve of S parameter with  $a$ .

On this basis, the digitization effect of college music education resources proposed in this paper is evaluated, and the evaluation results are obtained as shown in Table 1.

From the test results in Table 1, it can be seen that the digital system of music education resources in colleges and universities proposed in this paper has good effects and can effectively improve the processing quality of digital music resources in colleges and universities.

Num	Digital effects	Num	Digital effects
1	81.656	18	87.355
2	84.135	19	84.283
3	85.666	20	84.984
4	83.161	21	83.222
5	85.219	22	86.593
6	86.922	23	86.561
7	86.119	24	83.406
8	87.379	25	83.800
9	87.434	26	87.724
10	81.879	27	81.276
11	81.032	28	86.708
12	82.614	29	87.463
13	84.700	30	87.817
14	82.056	31	87.450
15	84.502	32	86.356
16	79.759	33	86.503
17	86.521	34	81.804

**Table 1:** Effect evaluation of the digital system of music education resources in colleges and universities.

#### 4 CONCLUSION AND FUTURE WORK

Professionalism is one of the key development principles that should be followed in the development of digital music classroom teaching assistant system. The application scope of the system is mainly classroom music teaching, which is an application scenario with high professional requirements, and the discipline of music itself pays great attention to sensory experience and quality. Because the system cannot reach the due level in terms of professionalism, the digital music classroom teaching assistant system is still in the trial stage. Its main functions include simulating piano playing, score editing, and score presentation, so there is still a lot of room for expansion. This paper uses digital technology to carry out digital processing of music education resources in colleges and universities. Through the experimental research, it can be seen that the digital system of music education resources in colleges and universities proposed in this paper has a good effect.

Huihui Ji, <https://orcid.org/0000-0002-7805-0222>



## REFERENCES

- [1] Calegario, F.; Wanderley, M. M.; Huot, S.; Cabral, G.; Ramalho, G.: A method and toolkit for digital musical instruments: generating ideas and prototypes, *IEEE MultiMedia*, 24(1), 2017, 63-71. <https://doi.org/10.1109/MMUL.2017.18>.
- [2] Tomašević, D.; Wells, S.; Ren, I. Y.; Volk, A.; Pesek, M.: Exploring annotations for musical pattern discovery gathered with digital annotation tools, *Journal of Mathematics and Music*, 15(2), 2021, 194-207. <https://doi.org/10.1080/17459737.2021.1943026>.
- [3] Serra, X.: The computational study of a musical culture through its digital traces, *Acta Musicologica*, 89(1), 2017, 24-44.
- [4] Gorbunova, I. B.; Petrova, N. N.: Digital Sets of Instruments in the System of Contemporary Artistic Education in Music: Socio-Cultural Aspect, *Journal of Critical Reviews*, 7(19), 2020, 982-989.
- [5] Partesotti, E.; Peñalba, A.; Manzolli, J.: Digital instruments and their uses in music therapy, *Nordic Journal of Music Therapy*, 27(5), 2018, 399-418. <https://doi.org/10.1080/08098131.2018.1490919>.
- [6] Babich, B.: Musical "Covers" and the Culture Industry: From Antiquity to the Age of Digital Reproducibility, *Research in Phenomenology*, 48(3), 2018, 385-407. <https://doi.org/10.1163/15691640-12341403>.
- [7] Gonçalves, L. L.; Schiavoni, F. L.: Creating Digital Musical Instruments with libmosaic-sound and Mosaicode, *Revista de Informática Teórica e Aplicada*, 27(4), 2020, 95-107. <https://doi.org/10.22456/2175-2745.104342>.
- [8] Gorbunova, I. B.: Music computer technologies in the perspective of digital humanities, arts, and researches, *Opcion*, 35(SpecialEdition24), 2019, 360-375.
- [9] Dickens, A.; Greenhalgh, C.; & Koleva, B.: Facilitating Accessibility in Performance: Participatory Design for Digital Musical Instruments, *Journal of the Audio Engineering Society*, 66(4), 2018, 211-219.
- [10] Vereshchahina-Biliavska, O. Y.; Cherkashyna, O. V.; Moskvichova, Y. O.; Yakymchuk, O. M.; & Lys, O. V.: Anthropological view on the history of musical art, *Linguistics and Culture Review*, 5(S2), 2021, 108-120. <https://doi.org/10.21744/lingcure.v5nS2.1334>.
- [11] Tabuena, A. C.: Chord-Interval, Direct-Familiarization, Musical Instrument Digital Interface, Circle of Fifths, and Functions as Basic Piano Accompaniment Transposition Techniques, *International Journal of Research Publications*, 66(1), 2020, 1-11. <https://doi.org/10.47119/IJRP1006611220201595>.
- [12] Anaya Amarillas, J. A.: Marketing musical: música, industria y promoción en la era digital, *INTERdisciplina*, 9(25), 333-335.
- [13] Scavone, G.; Smith, J. O.: A landmark article on nonlinear time-domain modeling in musical acoustics, *The Journal of the Acoustical Society of America*, 150(2), 2021, R3-R4. <https://doi.org/10.1121/10.0005725>.
- [14] Turchet, L.; West, T.; Wanderley, M. M.: Touching the audience: musical haptic wearables for augmented and participatory live music performances, *Personal and Ubiquitous Computing*, 25(4), 2021, 749-769. <https://doi.org/10.1007/s00779-020-01395-2>.
- [15] Stensæth, K.: Music therapy and interactive musical media in the future: Reflections on the subject-object interaction, *Nordic Journal of Music Therapy*, 27(4), 2018, 312-327. <https://doi.org/10.1080/08098131.2018.1439085>.